atmosphere

MDPI

Article

Long-Term Variability in Potential Evapotranspiration, Water Availability and Drought under Climate Change Scenarios in the Awash River Basin, Ethiopia

Mahtsente Tadese [1,*], Lalit Kumar [1] and Richard Koech [2]

[1] School of Environmental and Rural Science, University of New England (UNE), Armidale 2351, Australia; lkumar@une.edu.au

[2] Agriculture, Science, and Environment, Central Queensland University, Bundaberg Campus, QLD 4670, Australia; r.koech@cqu.edu.au

* Correspondence: mtadese@myune.edu.au

Received: 7 July 2020; Accepted: 17 August 2020; Published: 19 August 2020

Abstract: Understanding the hydrological processes of a watershed in response to climate change is vital to the establishment of sustainable environmental management strategies. This study aimed to evaluate the variability of potential evapotranspiration (PET) and water availability in the Awash River Basin (ARB) under different climate change scenarios and to relate these with long-term drought occurrences in the area. The PET and water availability of the ARB was estimated during the period of 1995–2009 and two future scenarios (2050s and 2070s). The representative concentration pathways (RCP4.5 and RCP8.5) simulations showed an increase in the monthly mean PET from March to August in the 2050s, and all the months in the 2070s. The study also identified a shortage of net water availability in the majority of the months investigated and the occurrence of mild to extreme drought in about 40–50% of the analysed years at the three study locations (Holetta, Koka Dam, and Metehara). The decrease in water availability and an increase in PET, combined with population growth, will aggravate the drought occurrence and food insecurity in the ARB. Therefore, integrated watershed management systems and rehabilitation of forests, as well as water bodies, should be addressed in the ARB to mitigate climate change and water shortage in the area.

Keywords: evapotranspiration; variability; water availability; drought; climate change

1. Introduction

Climate change and anthropogenic factors cause long-term variability in the meteorological parameters of a watershed, leading to changes in the hydrological cycle [1]. Precipitation and temperature are the major meteorological parameters that have a direct effect on the hydrological cycle. The change in precipitation and temperature influence water resources, land cover, and ecological sustainability. Consequently, such changes can significantly affect the spatial and temporal availability of water resources and the water balance [2–4].

Evapotranspiration (ET) is the critical climate variable that relates evaporation, latent heat flux, and transpiration [5–8]. The ET represents the amount of water that evaporates from water bodies and transpires from plants. It plays a significant role in surface runoff and groundwater prediction, water balance assessment, crop water requirement, and environmental water demand assessment [9–11]. Therefore, it is a vital component in hydrological water balance, global atmospheric system, water resource management, and design of hydrological structures [7,12,13]. The potential evapotranspiration (PET) is an indicator of the environmental demand for evapotranspiration, and is thus the widely accepted method of estimating evapotranspiration for hydrological assessment

purposes [14–16]. Previous studies used different methods to estimate PET, including empirical equations such as the Hargreaves method and the complicated energy-mass transfer models [17–20]. The Hargreaves method is a temperature-based method suitable for locations with limited hydro-climatology data [21,22]. This method calculates PET using a simplified equation requiring maximum and minimum temperature, recording year, and latitude [23].

The hydrological cycle illustrates the water movement and its storage within, above and below the Earth surface [24–26]. The major components of the hydrological cycle are precipitation, evapotranspiration, runoff and groundwater. The hydrological cycle of a watershed describes the water balance between the inflow of water as precipitation and upstream drainage, and outflow of water as evaporation, transpiration, downstream drainage and any internal storage [8,27]. When there is sufficient precipitation, the water supply may or may not be increased while the net water supply declines due to a decrease in precipitation. Water supply declines when temperature increases, which causes a higher evaporation rate and a rise in water demand. The changes in temperature, evaporation, and water demand have a significant effect on agriculture, energy production, and water usage in a watershed [7,10]. Furthermore, meteorological and hydrological droughts are the major environmental changes that occur due to long-term temperature and precipitation change. Drought indices can be used to investigate the occurrence of meteorological and hydrological drought. The Standardized Precipitation Index is the widely used drought index while Reconnaissance Drought Index and Streamflow Drought Index are the recently developed indices to analyse drought occurrence [28–31].

Understanding the impacts of climate change on the hydrological processes of a watershed is vital to the establishment of sustainable environmental management strategies aimed at improving water management [1]. The spatial and temporal variability of hydrological processes has a direct influence on agricultural and economic development. ET-based methods are used to provide valuable information on broad aspects such as ecology, hydrology, atmospheric science, agronomy, and carbon science of a watershed [7]. ET-based research has been conducted in different countries [32–34]; however, limited studies have been undertaken in Ethiopia, especially in the Awash River Basin (ARB). Therefore, this research aims to (a) evaluate the variability of potential evapotranspiration in ARB under different climate change scenarios, (b) predict the change in water availability in ARB, and (c) assess the long-term drought occurrence and relate it with the variability in PET and water availability. The investigative outcome of this research will help to design and establish sustainable water resources management in ARB.

2. Methodology

2.1. Study Area

The study was carried out in the Awash River Basin (ARB), Ethiopia (latitude 7°53′ N–12° N; longitude 37°57′ E–43°25′ E) (Figure 1). The ARB is one of the 12 river basins in Ethiopia, with an area of 112,000 km^2. A previous study by Ethiopia's Ministry of Environment, Forest and Climate Change (MEFCC) [35] indicated that the annual flow from this river basin was 4.9 billion cubic metres (BM^3). Most of the Ethiopian rivers show seasonality of water flows and heavy sediment load, and about 90% of their annual runoff occurs in the main rainy season, from July to September. The Awash River originates from Ginchi Town and ends at Lake Abee. The altitude of the ARB ranges from 210–4195 m above mean sea level, and the main Awash River has a length of 1250 km. The annual rainfall of the ARB ranges from 200–1800 mm [35], and the temperature ranges from 12–37 °C [36].

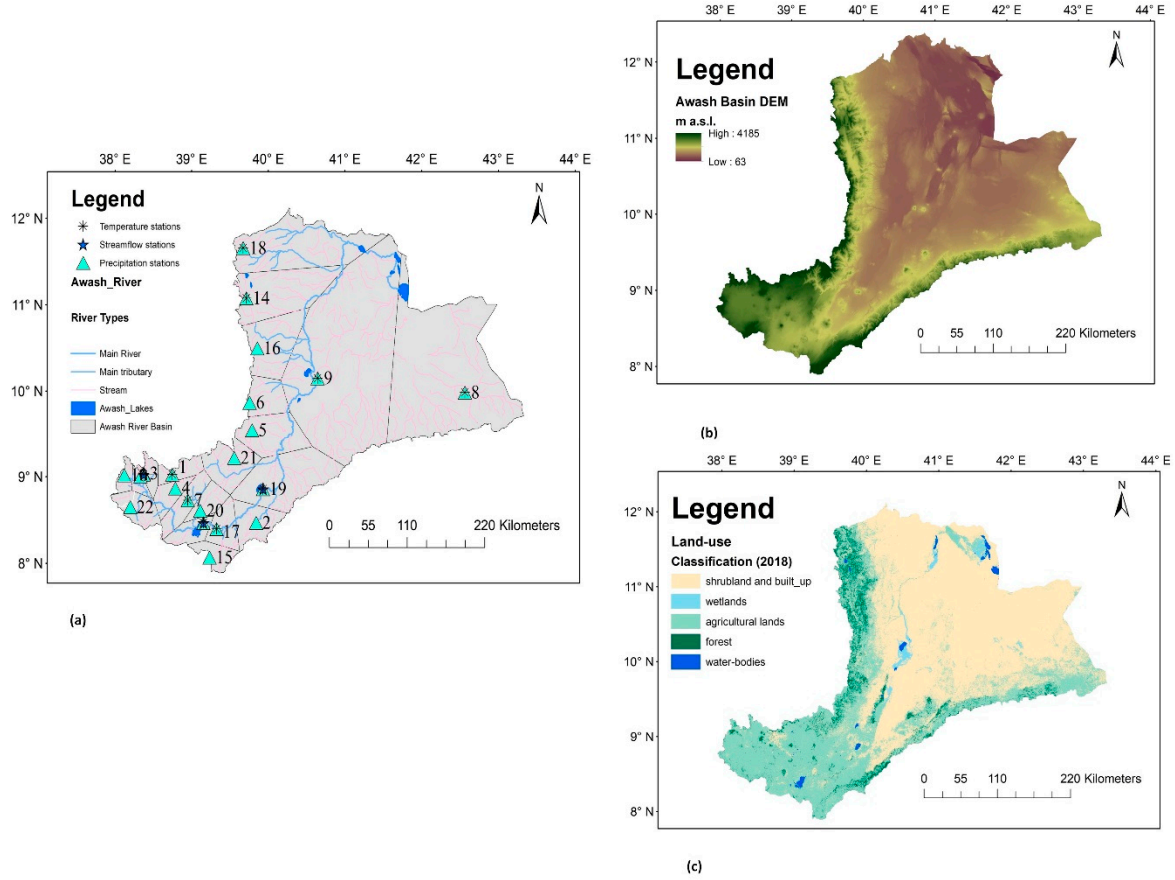

Figure 1. Map showing (**a**) the location of the study site and the meteorological stations, (**b**) digital Elevation Model (DEM) of the Awash River Basin (ARB), and (**c**) land-use classification of the ARB (2018) [37].

2.2. Dataset

The daily data of precipitation, temperature, and streamflow were collected from the National Meteorology of Ethiopia and Ethiopia's Ministry of Water, Irrigation, and Energy. In this study, 3, 10, and 22 stations were selected for streamflow, temperature, and precipitation data, respectively (Figure 1). The selection of the stations and the duration of the historical period were based on the availability of long-term data and minimum missing values. Fifteen years (1995–2009) was used for PET and water availability analysis as there was no decent data available after 2009, while 30 years (1986–2015) was taken for drought analysis. All the selected stations had less than 10% missing data. Thus, data from at least two or more representative stations in the Upper, Middle, and Lower parts of the basin were used in the study. The meteorological stations used in this study are shown in Table 1. The monthly average precipitation of the ARB was calculated by the Thiessen polygon method in ArcMap 10.4 using the twenty-two rainfall stations (Figure 1). The future precipitation and temperature were taken from two different General Climate models (HadGEM2_AO and GFDL_CM3) and three different Regional Climate models (CCLM, CNRM_RCA4, and MPI_RCA4) (Table 2). The Regional Climate Models (RCMs) and General Climate Models (GCMs) data were obtained from CORDEX Africa and WorldClim Version-1, respectively. The future period includes two scenarios: mid of 2041–2060 and 2060–2080 under two representative concentration pathways (RCP4.5 and RCP8.5). The GCM data was statistically downscaled and bias-corrected [38], while the RCM data was bias corrected using Climate Model data for hydrologic modelling (CMhyd) tool [39].

Table 1. Details of the meteorological stations in the Awash River Basin.

No	Stations	Longitude	Latitude	Elevation (m)	Variables	Duration
1	Addis Ababa Bole	38.75	9.03	2354	Precipitation, temperature	1995–2009
2	Addis Alem	38.38	9.04	2372	Precipitation	1995–2009
3	Akaki	38.79	8.87	2057	Precipitation	1995–2009
4	Abomassa	39.83	8.47	1630	Precipitation	1995–2009
5	Aliyu Amba	39.78	9.55	1805	Precipitation	1995–2009
6	Debre Zeyit	38.95	8.73	1900	Temperature, precipitation	1995–2009
7	Debre Sina	39.75	9.87	2800	Precipitation	1995–2009
8	Dire Dawa	42.53	9.97	1180	Temperature, precipitation	1995–2009
9	Ginchi	38.13	9.02	2132	Precipitation	1995–2009
10	Gewane	40.63	10.15	568	Temperature, precipitation	1995–2009
11	Holetta	38.38	9.03	2400	Streamflow, temperature, precipitation	1986–2009, 1986–2015
12	Koka Dam	39.15	8.47	1618	Streamflow, temperature, precipitation	1986–2009, 1986–2015
13	Kulumsa	39.23	8.07	2211	Precipitation	1995–2009
14	Kimoye	38.34	9.01	2150	Precipitation	1995–2009
15	Kombolcha	39.71	11.08	2341	Temperature, precipitation	1995–2009
16	Metehara	39.92	8.86	944	Streamflow, temperature, precipitation	1986–2009, 1986–2015
17	Majete	39.85	10.5	2000	Precipitation	1995–2009
18	Melkasa	39.32	8.4	1540	Temperature, precipitation	1995–2009
19	Merssa	39.67	11.66	1578	Temperature, precipitation	1995–2009
20	Mojo	39.11	8.61	1763	Precipitation	1995–2009
21	Shola Gebeya	39.55	9.22	2500	Precipitation	1995–2009
22	Tulu Bolo	38.21	8.65	2190	Precipitation	1995–2009

Table 2. List of climate models (General Climate Models (GCMs) and Regional Climate Models (RCMs)) used in this study [39].

No	Climate Model	Abbreviations (for This Study)	Organization	Resolution (°)
1	CNRM-CERFACS-CNRM-CM5_CLMcom-CCLM4-8-17	CCLM	Climate Limited Area Modeling (CLM) Community	0.44
2	MPI-M-MPI-ESM-LR_SMHI-RCA4	MPI_RCA4	MPI (Max Planck Institute), Germany	0.44
3	CNRM-CERFACS-CNRM-CM5_SMHI-RCA4	CNRM_RCA4	SMHI (Sveriges Meteorologiska och Hydrologiska Institute), Sweden	0.44
4	GFDL_CM3	GFDL_CM3	Geophysical Fluid Dynamics Laboratory	2.0 × 2.5
5	HadGEM2_AO	HadGEM2_AO	Met Office, Hadley Centre, United Kingdom	1.3 × 1.9

2.3. Data Analysis

2.3.1. Evapotranspiration

The daily historical temperature and precipitation data were arranged and checked for consistency and missing values in Microsoft Excel®. The summarized monthly and annual data were used in the historical and future period analysis. In this study, the DrinC (Drought Indices Calculator) software [31] was used to calculate the PET using the Hargreaves method. The DrinC is a user-friendly software widely used to calculate different drought indices and PET. The Hargreaves method uses temperature data to estimate PET, as shown in Equation (1) [40].

$$PET = 0.0023 \times RA \times \left(T^{\circ}\mathrm{C} + 17.8\right) \times TD^{0.05} \quad (1)$$

where *PET* represents a daily *PET* and *RA* is extra-terrestrial radiation in mm/day; *TD* is the mean of maximum temperature minus mean of minimum temperature ($T_{max} - T_{min}$) in degree Celsius, while T°C denotes the mean of maximum and minimum temperature ($T_{max} + T_{min}$)/2.

The historical PET (1995–2009) was calculated by the Hargreaves method in DrinC software for each of the 10 stations. The mean PET of the 10 stations was taken to analyse the variability of PET in the ARB. The maximum and minimum temperature data from five different GCMs and RCMs models were used to analyse the future PET of ARB. Statistically downscaled and bias-corrected GCMs data downloaded from WorldClim and the bias-correction for the RCMs data was performed by distribution mapping method using CMhyd tool [39]. The temporal variability of monthly and seasonal historical and future PET was evaluated using a graphical method in Microsoft Excel®.

2.3.2. Water Availability

The general water balance equation can be used to identify and model the water system using inflow and outflow of water in an area [8,24,27]. In this study, the balance between precipitation and potential evapotranspiration (Equation (2)) was used to estimate the amount of water that could be returned to the atmosphere, that is, net water available (NWA).

$$NWA = P - PET \quad (2)$$

where *NWA*, *P*, *and PET* denote the net water available, precipitation, and potential evapotranspiration, respectively.

The net water available in the watershed can be expressed as the total available water that can be in the form of runoff, soil moisture, and groundwater recharge. In this study, the monthly precipitation of ARB calculated using Thiessen polygon method was taken as precipitation of the area, while the monthly PET calculated using DrinC was considered as measure of evaporation. Then, these variables were used to estimate the net water available in the area, which includes the runoff and change in storage. The net monthly water availability was computed by deducting the monthly PET of the area from its corresponding monthly mean precipitation. The net water availability was calculated for the historical (1995–2009) and future periods (2050s and 2070s under RCP4.5 and RCP8.5) to analyse the monthly and seasonal variation of water availability in the ARB.

2.3.3. Drought Indices

Drought indices can be assessed using different indicators. In this study, a standardized precipitation index (SPI), reconnaissance drought index (RDI), and streamflow drought index (SDI) were used to analyse the occurrence and severity of hydrological drought at three locations within the ARB (Holetta, Koka Dam, and Metehara). The three locations were selected based on long-term data availability, and they represent the upper and middle part of ARB. The historical drought indices at Holetta, Koka Dam, and Metehara were calculated using DrinC software. The drought analysis was

carried out in 3, 6, and 12 months' time scale at the selected locations. The RDI and SPI were calculated for 30 years (1986–2015), while the SDI was analysed for 24 years (1986–2009) due to data availability.

Reconnaissance Drought Index (RDI)

The RDI is one of the accurate methods for agricultural drought analysis that incorporates two meteorological parameters, measured precipitation and calculated PET [41,42]. The RDI was used to detect the water deficit in a water system considering the inflow and outflow of water [43]. The RDI was calculated using Equations (4) [31].

$$\alpha_k^{(i)} = \frac{\sum_{j=1}^{k} P_{ij}}{\sum_{j=1}^{k} PET_{ij}},\ i = 1\ to\ N\ and\ j = 1\ to\ k \tag{3}$$

where PET_{ij} *and* P_{ij} denote the potential evapotranspiration and precipitation in the *j*th of month and *i*th of year, respectively, and N is the total number of years of available data.

Previous studies showed that α_k (Equation (3)) follow satisfactory lognormal and gamma distributions in wide range of locations and timescales [44,45] and by assuming lognormal distribution RDI_{st} can be calculated as:

$$RDI_{st}^{i} = \frac{y^{(i)} - \overline{y}}{\hat{\sigma}_y} \tag{4}$$

where $y^{(i)}$ is the ln $(\alpha_k^{(i)})$, and $\overline{y}$ & $\hat{\sigma}_y$ denote its mean and standard deviation, respectively.

Standardized Precipitation Index (SPI)

The SPI has been used in a number of studies [46–49]. It uses the gamma distribution and cumulative probability to detect a drought event and is calculated at several time scales [31]. In this study, SPI was calculated using DrinC software.

Streamflow Drought Index (SDI)

The SDI is a recently developed drought index used to detect hydrological drought. In this study, the SDI was calculated using Equations (5) and (6) [31].

$$V_{i,k} = \sum\nolimits_{j=1}^{3k} Q_{i,j}\ \ i = 1,2,3,\ldots; j = 1,2,3,\ldots,12\ and\ k = 1,2,3,4 \tag{5}$$

$$SDI_{i,k} = \frac{V_{i,k} - \overline{V}_k}{s_k}\ \ i = 1,2,\ldots,k = 1,2,3,\ and\ 4 \tag{6}$$

where $Q_{i,j,}$*and* $V_{i,k}$ denote the monthly streamflow and cumulative streamflow in the *i*th year and *k*th reference period, respectively; *i and j* denote the hydrological year and month of the data, respectively. The *k* period refers to *k* = 1 (October–December), *k* = 2 (October–March), *k* = 3 (October–June), and *k* = 4 (October–September); $\overline{V}_k$ is the mean, and s_k is the standard deviation of cumulative streamflow.

The classification of drought indices (Table 3; Table 4) was undertaken according to previous studies [31,46,50–52]. In this study, the near-normal category for RDI and SPI were separated into two groups as normal wet from 0 to 1.0, and mild dry from 0 to −1.0.

Table 3. Reconnaissance drought index (RDI)- and standardized precipitation index (SPI)-based drought classification.

RDI and SPI Range	Description
≤−2.0	Extremely dry
−2.0 to −1.5	Severely dry
−1.5 to −1.0	Moderately dry
−1.0 to 1.0	Near Normal

Table 4. Streamflow drought index (SDI)-based hydrological drought classification.

SDI Range	Description
<−2.0	Extreme drought
−2.0 to −1.5	Severe drought
−1.5 to −1.0	Moderate drought
−1.0 to 0	Mild drought
≥0	Non-drought

3. Results

3.1. Potential Evapotranspiration (PET)

Figure 2a shows the percentage of change in potential evapotranspiration (PET) in 2050s RCP4.5 using five different climate models. Most of the climate model simulations have a similar pattern with historical PET. The change in PET showed a similar temporal trend for more than four model simulations in half of the twelve months. The positive value indicated an increase in PET, while the negative value showed a decrease in PET. The 2050s RCP4.5 simulation indicated an increase in mean monthly PET from March to August (Figure 2a). However, a decrease in the mean monthly PET was indicated from September to December. During this period, the increase in mean PET ranged from 3–43%, while the decrease rate ranged from 2–10%. The higher increase occurred during June, whereas a higher decrease was detected in December. The percentage of change in PET in 2050s RCP8.5 using different climate model simulations are shown in Figure 2b. In this period, the change in PET showed a similar temporal trend for more than four model simulations in 8 of the 12 months, while 4 of the months showed a different temporal trend. The 2050s RCP8.5 monthly PET showed an increase from March to September and a decrease for the other months (Figure 2b). The increase in mean PET ranged from 3–46%, and the highest increase was detected in June. Conversely, the highest decrease was identified in December (−12%).

Figure 2c shows the change in monthly PET (%) in 2070s RCP4.5 using GCMs and RCMs simulations. The change in PET showed a similar temporal trend for more than four model simulations in eight of the twelve months. The 2070s RCP4.5 simulation showed a decrease in mean monthly PET only in December (−9%) and February (−3%). The increase in mean monthly PET was detected in the rest of the months with a range of 2–35%. The highest decrease and increase were indicated in December and June, respectively. The 2070s RCP8.5 monthly change in PET of different GCMs and RCMs simulations are shown in Figure 2d. The change in PET showed a similar temporal trend for more than four model simulations in nine of the twelve months. For only three of the months, the future simulations indicated a different temporal trend. The 2070s RCP8.5 simulation revealed an increase in mean monthly PET in all the months except a slight decrease in December (Figure 2d). The increase in mean monthly PET ranged from 3–55%, and the highest increase was detected in June.

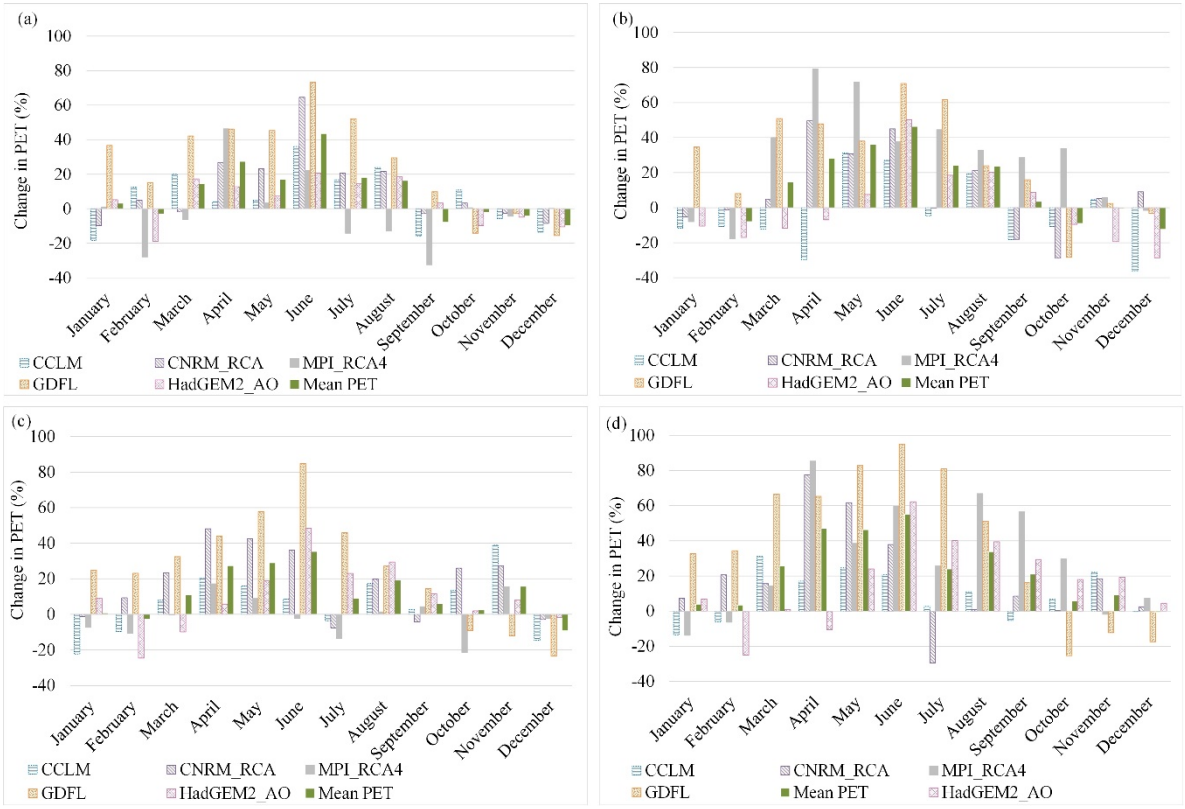

Figure 2. Percentage of change in potential evapotranspiration (PET) in Awash River Basin (ARB) using different GCMs simulations (GDFL and HadGEM2_AO) and RCMs simulations (CCLM, MPI_RCA4, and CNRM_RCA). Future simulations: (**a**) 2050s RCP4.5 (**b**) 2050s RCP8.5 (**c**) 2070s RCP4.5 and (**d**) 2070s RCP8.5.

3.2. Net Water Availability

Figures 3 and 4 show the net monthly water availability of ARB using different GCMs and RCMs simulations. The net water availability using all the five climate models indicated a similar pattern with the historical period. Almost all five model simulations indicated a positive value in net water availability during July and August (Figure 3). However, the negative value was shown in the rest of the months in most of the simulations and historical period. In September, the net water availability showed a negative value but higher than the historical period. Similarly, March and April exhibited a negative value but lower than the historical period in most of the simulations. The highest decrease in water availability was 143.94 mm in 2050s RCP4.5, 128.82 mm in 2050s RCP8.5, and 145.87 mm in 2070s RCP8.5 simulation (Figure 4). However, the higher increase in water availability was 67.73, 54.79, and 71.04 mm in the 2050s RCP4.5, 2050s RCP8.5, and 2070s RCP8.5 simulations, respectively. On the other hand, the 2070s RCP8.5 showed the highest deficit of 135.46 mm in November and the highest increase of 72.42 mm in July.

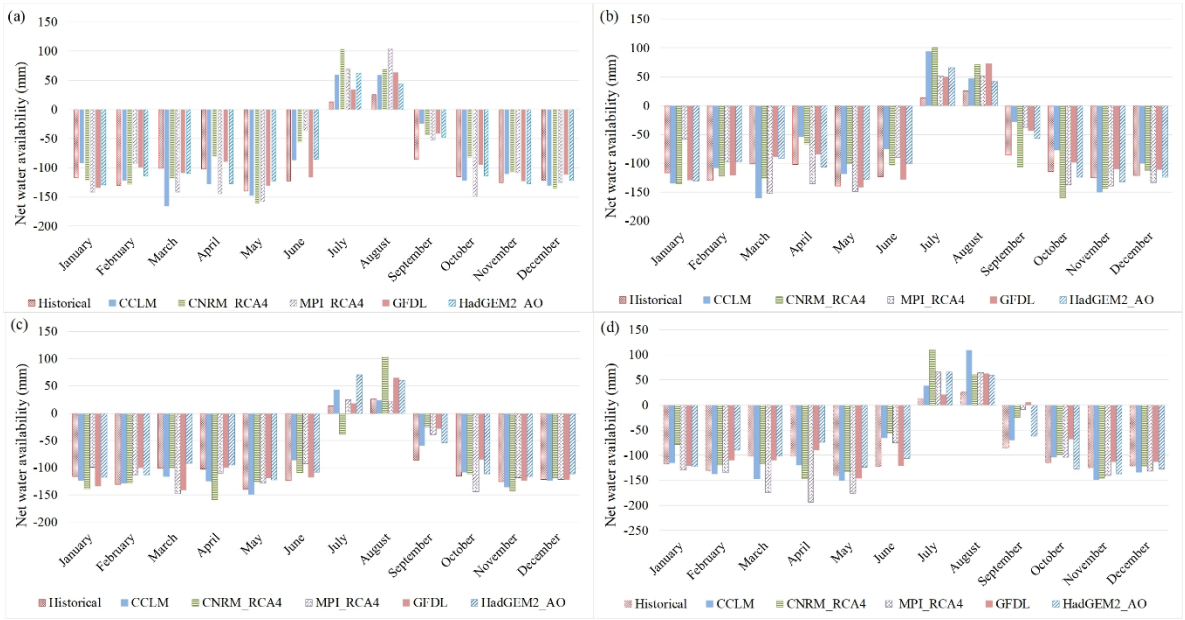

Figure 3. The net water availability of Awash River Basin during the historical period (1995–2009) and future GCMs simulations (GFDL and HadGEM2_AO) and RCMs simulations (CCLM, MPI_RCA4, and CNRM_RCA4). Future simulations: (**a**) 2050s RCP4.5 (**b**) 2070s RCP4.5 (**c**) 2050s RCP8.5, and (**d**) 2070s RCP8.5.

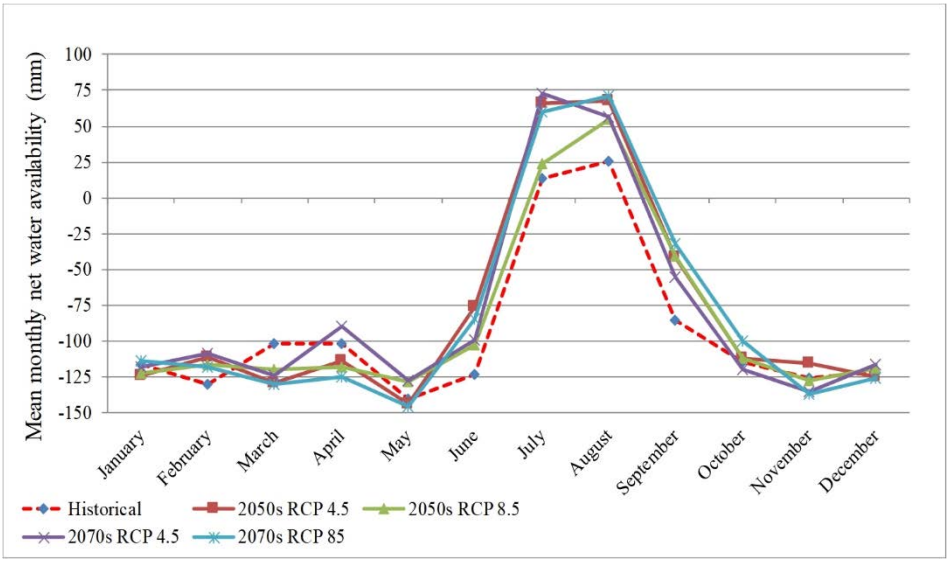

Figure 4. The historical (1995–2009) and future mean monthly net water availability of Awash River Basin under RCP4.5 and RCP8.5 simulations.

3.3. Drought Index

According to the United Nations Environment Programme [53] aridity index, Koka Dam (aridity index = 0.45) and Metehara (aridity index = 0.24) are classified as semi-arid, while Holetta (aridity index = 0.64) is identified as dry sub-humid. The 3 month, 6 month, and 12 month timescale SPI and RDI showed a similar pattern, with correlation ranging from 0.93–0.99 in all the three locations.

The 12 months Drought Indices

Figure 5 shows the 12 months SPI, RDI, and SDI at the three locations (Holetta, Koka Dam, and Metehara). The 12 months SPI showed a dry period of mild to extreme dry at 43% of the analysed years at Holetta and Metehara while it was 47% at Koka Dam. Moreover, the 12 months RDI showed

a dry period at 40%, 50%, and 43% of the analysed years at Holetta, Koka Dam, and Metehara, respectively. At Holetta, the severe drought occurred in 2009 (RDI = −1.9) and the extreme drought occurred in 2015 (RDI = −3.3) (Figure 5a). The SPI and RDI at Holetta showed a continuous dry period from 2002 to 2005. From 1997 to 2001, a relatively continuous wet period was shown at Koka Dam while a severe and extreme drought occurred in 1987 (RDI = −1.6) and 1986 (RDI = −2.4), respectively (Figure 5b). Considering the RDI value, the extreme drought at Metehara occurred in 2002 (RDI = −2.5) and 2015 (RDI = −2.8) (Figure 5c). Furthermore, the 12 month SDI indicated a mild to moderate drought at 58%, 50%, and 46% of the analysed years at Holetta, Koka Dam, and Metehara, respectively. The extreme drought occurred in 1988 (SDI = −2.15) and 2009 (SDI = −2.44) at Koka Dam, and in 1987 (SDI = −2.03) and 1988 (SDI = −2.3) at Metehara. A continuous mild drought occurred at Metehara from 1987–1989 and 2002–2005.

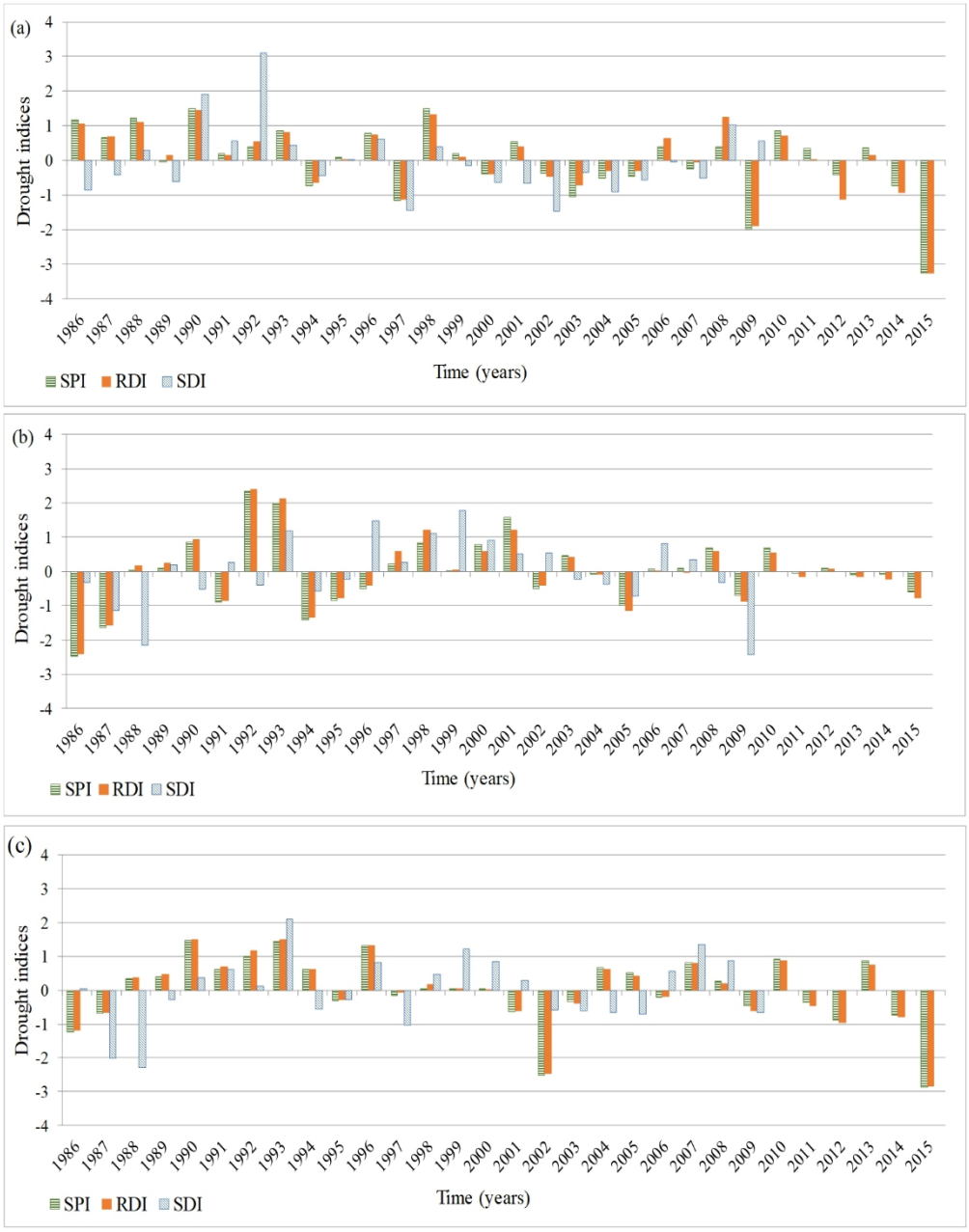

Figure 5. The 12 months drought indices (SPI, RDI, and SDI) at three locations; (**a**) Holetta, (**b**) Koka Dam, and (**c**) Metehara. SPI and RDI period: 1986–2015, SDI period: 1986–2009.

The 6 months Drought Indices

The 6 month SPI, RDI, and SDI at Holetta, Koka Dam, and Metehara are shown in Appendix A. The 6 month analysis considered two seasons: (i) October–March and (ii) April–September. The 6 month SPI, RDI, and SDI indicated a mild to extreme drought at 40–50% of the analysed years at Holetta, Koka Dam, and Metehara, except for the SDI at Holetta, which showed a dry period at 54–58% of the analysed years. At Holetta, a continuous dry period was shown from 2003–2007 during the first season, and an extreme drought occurred in 2012 (RDI = −3.3) and 2015 (RDI = −3.0) during the first and second seasons, respectively (Appendix A). At Koka Dam, the extreme drought occurred in 2012 (RDI = −2.2) and 1986 (RDI = −2.4) during the first and second seasons, respectively. Moreover, a severe drought was shown in 2015 (RDI = −1.9) during the first season. At Metehara, a continuous mild drought was shown from 1986–1988 during the first season, and then, an improvement has been observed. However, in 2000, a mild drought started and became severe in 2009 (RDI = −1.79), 2011 (RDI = −1.67), 2012 (RDI = −1.73), and 2015 (RDI = −1.74) (Appendix A). In addition, an extreme drought was shown in 1994 (RDI = −2.1), 2002 (RDI = −2.7), and 2015 (RDI = −2.6). A continuous mild to moderate drought occurred at Holetta from 1999–2005, at Koka Dam from 2003–2007, and Metehara from 2002–2005. An extreme streamflow drought occurred in 2002 (SDI = −2.4) at Holetta, in 1988 (SDI = −2.1) and 2009 (SDI = −2.2) at Koka Dam, and in 1988 (SDI = −2.8) at Metehara. The 6 month hydrological drought analysis showed the majority of the dry periods at Holetta, Koka Dam, and Metehara were mild droughts.

The 3 months Drought Indices

The 3 month drought analysis was performed for four seasons: (i) October–December, (ii) January–March, (iii) April–June, and (iv) July–September. The 3 month SPI and RDI result indicated a negative value at 40–53%, 43–53%, and 33–60% of the analysed years at Holetta, Koka Dam, and Metehara, respectively (Appendix B). At Holetta, the extreme drought occurred in 1989, 1991, 2000, 2002, 2004, 2008, 2009, 2012, and 2015 during one of the seasons. The severe and extreme drought existed at least in one of the seasons in 1986, 1987, 1988, 1991, 2007, and 2009 at Koka Dam. At Metehara, the severe and extreme drought occurred in 1987, 1989, 1995, 2000, 2002, 2008, 2012, and 2015 during one of the seasons. Considering the hydrological drought, about 54–67%, 50–63%, and 33–58% of the analysed years indicated a mild to extreme drought at Holetta, Koka Dam, and Metehara, respectively (Appendix B). A majority of the dry periods in all the three locations were mild drought and extreme drought occurred in 2002 (SDI = −2.6) at Holetta, in 1988 (SDI = −2.1) and 2009 (SDI = −2.1) at Koka Dam, and in 1987 (SDI = −2.6), 1988 (SDI = −3.2) and 1989 (SDI = −2.4) at Metehara. The variability of 3 month hydrological drought indicated a continuous mild drought in the majority of the analysed years, at least in one of the seasons in all the three locations.

4. Discussion

The change in monthly PET showed a similar pattern and temporal trend in most of the simulations undertaken using GCMs and RCMs. However, there was still some difference in the temporal trend in a few months under different model simulations. This indicated the existence of uncertainty in model simulations and the importance of using more than one model in order to increase the accuracy of the predictions. The 2050s RCP4.5 analysis indicated an increase in mean monthly PET from March to August. Similarly, in the 2050s RCP8.5, the monthly PET increased from March to September. The periods of March–May (MAM) and June–September (JJAS) are the two main rainfall seasons as well as the main rain-fed agricultural seasons in Ethiopia [54,55]. The 2050s RCP4.5 and RCP8.5 simulations showed an increase in the monthly PET during these seasons in ARB. This is likely to have a negative effect on agricultural productivity and irrigation management of the basin. Moreover, the crop water requirement and ecological water demand of the ARB will be influenced due to changes in PET. With inadequate water availability to satisfy the crop water demand, the growth of crops would be affected especially in the early and development stages which might result in crop failure due to agricultural drought.

Furthermore, the 2070s RCP4.5 simulations indicated an increase in mean monthly PET in all months except December and February. The mean monthly PET continued to increase in 2070s under RCP8.5 in all the months except December. The increase rate ranged from 3% to 55% in the 2050s and 2070s simulations, while the decrease rate ranged from 3% to 12%. This showed that an increased rate was about four times the decrease rate. Therefore, the increase in mean monthly PET was more significant than the decrease. The increase of monthly PET during most of the months might have a negative impact on the water management system, including irrigated and rain-fed agriculture in the ARB. The Awash basin is one of the most densely populated and intensively used basins in Ethiopia [35]. In the basin, large irrigation schemes and hydropower generation plants provide hydropower energy and water supply for different towns and cities. Previous studies showed the vulnerability of ARB to climate variability and water stress during agricultural seasons [56–58]. Moreover, the study by Tadese et al. [37] noted a 25% loss of forest and an expansion of cropland by 15% in 2018, which will have a significant influence on the hydrological process in ARB. Thus, the climate variability and land-use change in ARB is highly likely to intensify the increase in PET in the basin. An increase in PET could be a challenge in crop production especially in dry areas as it leads to an increase in crop water requirement and water demand. Similarly, previous studies have indicated the critical role of evapotranspiration on surface runoff, water budget, irrigation management, and environmental water system [7,10,13,14]. Integrated water management can help to boost crop productivity and improve water availability of the watershed by integrating land and water resources management, social and economic development. Therefore, integrated water management systems and sustainable climate change mitigation strategies are necessary for ARB to cope with these changes in PET.

The simulated net water availability in ARB indicated a negative value in most of the months using different climate models. This might be due to the topography and vegetation coverage of ARB. Moreover, about half of the basin area is covered with shrubland, barren areas, and drylands having higher evaporation losses, especially in the Lower and Middle Awash. Results from this study showed decreased net water availability in March and April and continues to decline under future simulations. Similarly, May and June showed a negative value during historical and future periods. A higher decrease was detected in most of the model simulations during May. The lower water availability from March to May is likely to have a significant impact on crop productivity as this is one of the main seasons for both irrigated and rain-fed agriculture in the ARB. Similarly, the study by [58] identified a decrease of water availability in ARB during most of the months.

On the other hand, the net water availability in July and August was positive and showed an improvement under future simulations. This suggests that during these months, the amount of water available for runoff, soil moisture, and groundwater recharge would be more than what would be expected in the other months. Furthermore, most of the runoff occurred during July and August, which coincides with Ethiopia's main rainy season. The excess water may be diverted, harvested, or stored and made available for future use and groundwater recharge. Thus, small and large diversions, dams, and reservoirs are essential in areas like the ARB, which have only a few months with higher rainfall and no rainfall or minimal rainfall during most of the other months. Future water management strategies in the ARB should focus on these important aspects.

The 6 month and 12 month RDI and SPI analyses indicated a dry period from mild to extreme drought at 40–50% of the analysed years. The SDI analysis also showed a hydrological drought at about half of the analysed years. The majority of these droughts were mild, and occurred after mostly 2001. Even though it was a mild drought, the continued occurrence might lead to severe drought and water stress in the long-run unless an appropriate water management system is established at the early stages. The ARB is one of the Ethiopian basins that is highly susceptible to hydrological variability [59] with frequent occurrence of drought [35,60,61]. The result of this is that there could be significant negative impact on crop production and food security for the increasing population in the area. The decrease in water availability and an increase in PET, combined with population growth, will aggravate the drought occurrence and food insecurity in the ARB, especially in the Lower and

Middle Awash, as the wider area was classified as arid and semi-arid with minimum forest coverage and high evaporation loss. Therefore, integrated watershed management systems and rehabilitation of forests, as well as water bodies, should be addressed in order to mitigate climate change and water shortage in the area.

5. Conclusions

This study aimed to evaluate the variability of potential evapotranspiration (PET) and water availability in the Awash River Basin (ARB) under different climate change scenarios and to relate these with long-term drought occurrences in the area. The PET and water availability of ARB were estimated using DrinC software and water balance approach during the periods 1995–2009 and two future years (2050s and 2070s). In addition, the variability of drought in ARB was evaluated using three drought indices (RDI, SPI, and SDI). Based on the findings of this study, the representative concentration pathways (RCP4.5 and RCP8.5) simulations showed an increase in the monthly mean PET from March to August in the 2050s, and almost all the months in the 2070s. The study also found that the increase rate was considerably higher than the decrease rate. The change in PET has a significant role in the water balance system, including surface runoff, water resources management, crop, and ecological water demand. Therefore, the increase in monthly PET will have a critical effect on the overall crop productivity and water management of the ARB.

Furthermore, the monthly net water availability of the ARB showed a shortage of water in the majority of the months investigated, and the higher decrease was detected from March to May. This has a direct influence on irrigated and rain-fed agriculture in the basin. Moreover, the long-term drought analysis showed the existence of mild to extreme meteorological and hydrological drought at about 40–50% of the analysed years at the three study locations (Holetta, Koka Dam, and Metehara). Generally, the change in PET and net water availability showed the deficit of water during most of the months and frequent occurrence of the mild drought periods in ARB. The findings of this study are an indicator of the existence of water deficit and drought in the ARB, and crucial attention should be given to sustainable watershed management and climate change mitigation strategies in the ARB, especially in the Lower and Middle parts. Food security and sustainability of agricultural production in the ARB could be considerably exacerbated with a growing population in the ARB and the demand to produce more from reduced water availability unless necessary action is taken as early as possible.

Author Contributions: L.K.: conceptualization, validation, resources, writing—review and editing, supervision, project administration, funding acquisition. R.K.: investigation, validation, writing—review and editing, visualization, supervision. M.T.: conceptualization, methodology, formal analysis, investigation, validation, data curation, writing—original draft preparation, visualization. All authors have read and agreed to the published version of the manuscript.

Funding: The first author obtained research support from the University of New England through the International Postgraduate Research Award.

Acknowledgments: The authors acknowledge the University of New England in Australia, and Awash Basin Authority, Ethiopian National Meteorological Agency, and EIAR for their assistance.

Conflicts of Interest: There is no conflict of interest with the authors.

Appendix A

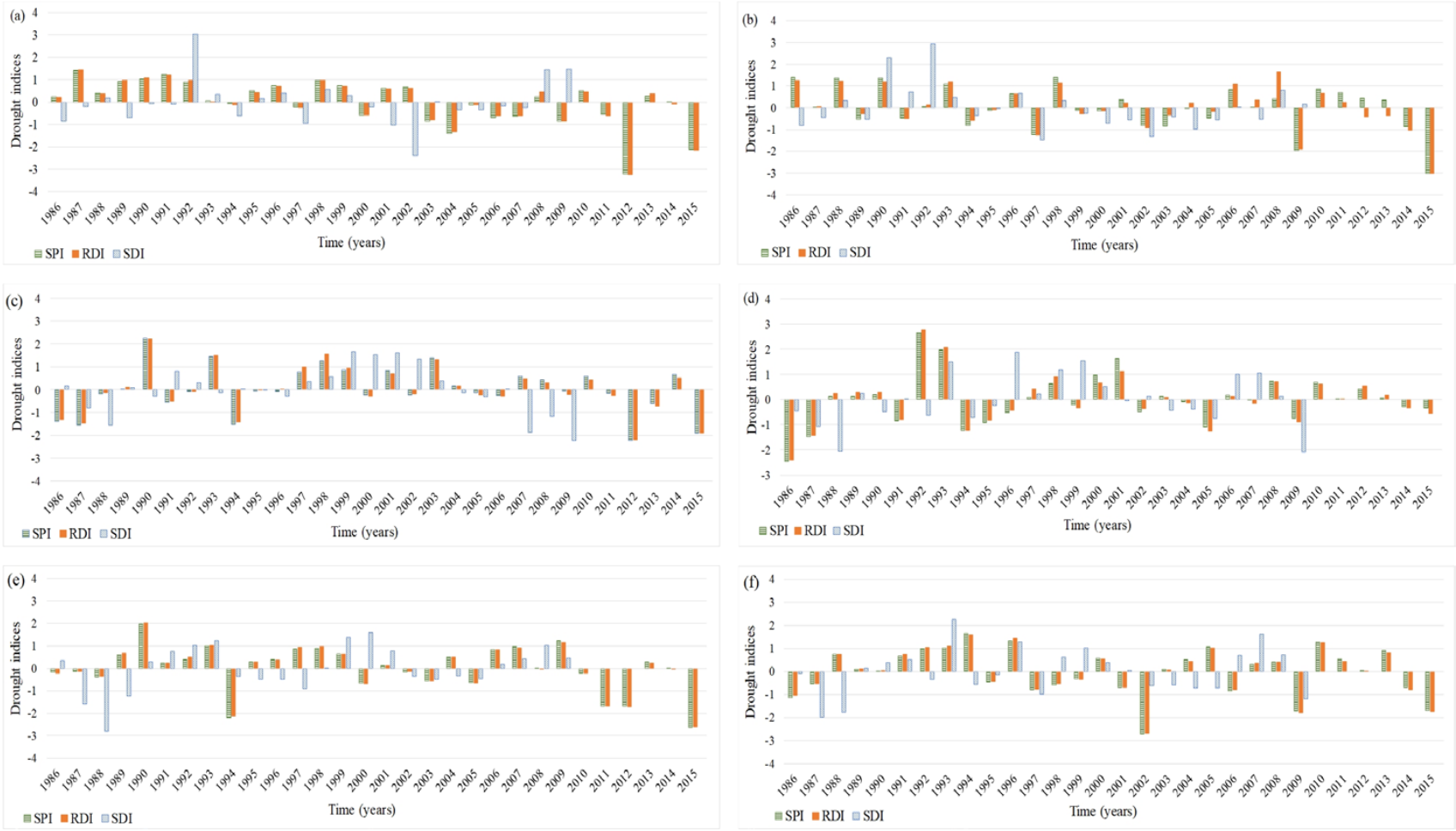

Figure A1. The 6 months drought indices (SPI, RDI, and SDI) at three locations during two seasons (i) October–March and (ii) April–September. Locations (**a**) Holetta first season (**b**) Holetta second season (**c**) Koka Dam first season (**d**) Koka Dam second season (**e**) Metehara first season and (**f**) Metehara second season. SPI and RDI period: 1986–2015, SDI: 1986–2009.

Appendix B

Table A1. The 3 months drought occurrence (%) based on SPI, RDI, and SDI values at three locations during four seasons: (i) October–December (ii) January–March (iii) April–June, and (iv) July–September.

3 Months First Season						
Locations	**Index**	**Drought Occurrence (%)**				**Total**
		Mild	**Moderate**	**Severe**	**Extreme**	
Holetta	SPI	36.7	10.0	6.7	0.0	53.3
	RDI	30.0	13.3	6.7	0.0	50.0
	SDI	50.0	0.0	0.0	4.2	54.2
Koka Dam	SPI	50.0	0.0	0.0	0.0	50.0
	RDI	53.3	0.0	0.0	0.0	53.3
	SDI	45.8	0.0	12.5	0.0	58.3
Metehara	SPI	46.7	6.7	6.7	0.0	60.0
	RDI	46.7	6.7	6.7	0.0	60.0
	SDI	33.3	12.5	0.0	4.2	50.0
3 Months Second Season						
Locations	**Index**	**Drought Occurrence (%)**				**Total**
		Mild	**Moderate**	**Severe**	**Extreme**	
Holetta	SPI3	23.3	6.7	6.7	3.3	40.0
	RDI3	23.3	6.7	6.7	3.3	40.0
	SDI3	62.5	0.0	0.0	4.2	66.7
Koka Dam	SPI3	33.3	13.3	0.0	0.0	46.7
	RDI3	30.0	13.3	0.0	0.0	43.3
	SDI3	29.2	16.7	0.0	4.2	50.0
Metehara	SPI3	20.0	3.3	10.0	0.0	33.3
	RDI3	20.0	3.3	10.0	0.0	33.3
	SDI3	16.7	4.2	4.2	8.3	33.3
3 Months Third Season						
Locations	**Index**	**Drought Occurrence (%)**				**Total**
		Mild	**Moderate**	**Severe**	**Extreme**	
Holetta	SPI	33.3	3.3	6.7	3.3	46.7
	RDI	30.0	13.3	3.3	3.3	50.0
	SDI	54.2	0.0	0.0	4.2	58.3
Koka Dam	SPI	40.0	6.7	6.7	0.0	53.3
	RDI	40.0	6.7	6.7	0.0	53.3
	SDI	41.7	4.2	4.2	4.2	54.2
Metehara	SPI	36.7	20.0	0.0	0.0	56.7
	RDI	36.7	20.0	0.0	0.0	56.7
	SDI	29.2	4.2	4.2	4.2	41.7

Table A1. *Cont.*

3 Months Fourth Season						
Locations	**Index**	**Drought Occurrence (%)**				**Total**
		Mild	**Moderate**	**Severe**	**Extreme**	
Holetta	SPI	33.3	10.0	0.0	3.3	46.7
	RDI	40.0	6.7	0.0	3.3	50.0
	SDI	45.8	12.5	0.0	0.0	58.3
Koka Dam	SPI	40.0	3.3	3.3	3.3	50.0
	RDI	26.7	10.0	3.3	3.3	43.3
	SDI	54.2	4.2	4.2	0.0	62.5
Metehara	SPI	26.7	13.3	3.3	3.3	46.7
	RDI	23.3	13.3	3.3	3.3	43.3
	SDI	41.7	12.5	0.0	4.2	58.3

References

1. Mohammed, R.; Scholz, M. Climate Variability Impact on the Spatiotemporal Characteristics of Drought and Arid ityin Arid and Semi-Arid Regions. *Water Resour. Manag.* **2019**, *33*, 5015–5033. [CrossRef]
2. Chen, H.; Guo, S.; Xu, C.-Y.; Singh, V.P. Historical temporal trends of hydro-climatic variables and runoff response to climate variability and their relevance in water resource management in the Hanjiang basin. *J. Hydrol.* **2007**, *344*, 171–184. [CrossRef]
3. Leta, O.T.; El-Kadi, A.I.; Dulai, H.; Ghazal, K.A. Assessment of climate change impacts on water balance components of Heeia watershed in Hawaii. *J. Hydrol. Reg. Stud.* **2016**, *8*, 182–197. [CrossRef]
4. Kusangaya, S.; Warburton, M.L.; Van Garderen, E.A.; Jewitt, G.P. Impacts of climate change on water resources in southern Africa: A review. *Phys. Chem. Earth Parts A/B/C* **2014**, *67*, 47–54. [CrossRef]
5. Ehlers, E.; Krafft, T. *German Global Change Research*; National Committee on Global Change Research: Bonn, Germany, 1998; p. 130.
6. Thomas, A. Spatial and temporal characteristics of potential evapotranspiration trends over China. *Int. J. Climatol. A J. R. Meteorol. Soc.* **2000**, *20*, 381–396. [CrossRef]
7. Fisher, J.B.; Melton, F.; Middleton, E.; Hain, C.; Anderson, M.; Allen, R.; McCabe, M.F.; Hook, S.; Baldocchi, D.; Townsend, P.A. The future of evapotranspiration: Global requirements for ecosystem functioning, carbon and climate feedbacks, agricultural management, and water resources. *Water Resour. Res.* **2017**, *53*, 2618–2626. [CrossRef]
8. Peters, T. *Water Balance in Tropical Regions*; Springer: Berlin/Heidelberg, Germany, 2016; pp. 391–403. [CrossRef]
9. Djaman, K.; Koudahe, K.; Ganyo, K.K. Trend analysis in annual and monthly pan evaporation and pan coefficient in the context of climate change in togo. *J. Geosci. Environ. Prot.* **2017**, *5*, 41–56. [CrossRef]
10. Muhammad, M.K.I.; Nashwan, M.S.; Shahid, S.; Ismail, T.B.; Song, Y.H.; Chung, E.-S. Evaluation of Empirical Reference Evapotranspiration Models Using Compromise Programming: A Case Study of Peninsular Malaysia. *Sustainability* **2019**, *11*, 4267. [CrossRef]
11. Lang, D.; Zheng, J.; Shi, J.; Liao, F.; Ma, X.; Wang, W.; Chen, X.; Zhang, M. A comparative study of potential evapotranspiration estimation by eight methods with FAO Penman–Monteith method in southwestern China. *Water* **2017**, *9*, 734. [CrossRef]
12. Djaman, K.; Balde, A.B.; Sow, A.; Muller, B.; Irmak, S.; N'Diaye, M.K.; Manneh, B.; Moukoumbi, Y.D.; Futakuchi, K.; Saito, K. Evaluation of sixteen reference evapotranspiration methods under sahelian conditions in the Senegal River Valley. *J. Hydrol. Reg. Stud.* **2015**, *3*, 139–159. [CrossRef]
13. Tukimat, N.N.A.; Harun, S.; Shahid, S. Comparison of different methods in estimating potential evapotranspiration at Muda Irrigation Scheme of Malaysia. *J. Agric. Rural Dev. Trop. Subtrop. (JARTS)* **2012**, *113*, 77–85.

14. Lu, J.; Sun, G.; McNulty, S.G.; Amatya, D.M. A comparison of six potential evapotranspiration methods for regional use in the Southeastern United States 1. *JAWRA J. Am. Water Resour. Assoc.* **2005**, *41*, 621–633. [CrossRef]
15. Douglas, E.M.; Jacobs, J.M.; Sumner, D.M.; Ray, R.L. A comparison of models for estimating potential evapotranspiration for Florida land cover types. *J. Hydrol.* **2009**, *373*, 366–376. [CrossRef]
16. Pan, S.; Xu, Y.-P.; Xuan, W.; Gu, H.; Bai, Z. Appropriateness of potential evapotranspiration models for climate change impact analysis in Yarlung Zangbo River basin, China. *Atmosphere* **2019**, *10*, 453. [CrossRef]
17. Khoshravesh, M.; Sefidkouhi, M.A.G.; Valipour, M. Estimation of reference evapotranspiration using multivariate fractional polynomial, Bayesian regression, and robust regression models in three arid environments. *Appl. Water Sci.* **2017**, *7*, 1911–1922. [CrossRef]
18. McMahon, T.A.; Peel, M.C.; Lowe, L.; Srikanthan, R.; McVicar, T.R. Estimating actual, potential, reference crop and pan evaporation using standard meteorological data: A pragmatic synthesis. *Hydrol. Earth Syst. Sci.* **2013**, *17*, 1331–1363. [CrossRef]
19. Hosseinzadeh Talaee, P. Performance evaluation of modified versions of Hargreaves equation across a wide range of Iranian climates. *Meteorol. Atmos. Phys.* **2014**, *126*, 65–70. [CrossRef]
20. Xu, C.-Y.; Singh, V. Cross comparison of empirical equations for calculating potential evapotranspiration with data from Switzerland. *Water Resour. Manag.* **2002**, *16*, 197–219. [CrossRef]
21. Berti, A.; Tardivo, G.; Chiaudani, A.; Rech, F.; Borin, M. Assessing reference evapotranspiration by the Hargreaves method in north-eastern Italy. *Agric. Water Manag.* **2014**, *140*, 20–25. [CrossRef]
22. Li, Z.; Yang, Y.; Kan, G.; Hong, Y. Study on the applicability of the Hargreaves potential evapotranspiration estimation method in CREST distributed hydrological model (Version 3.0) applications. *Water* **2018**, *10*, 1882. [CrossRef]
23. Hargreaves, G.H.; Samani, Z.A. Reference crop evapotranspiration from temperature. *Appl. Eng. Agric.* **1985**, *1*, 96–99. [CrossRef]
24. Edwards, P.J.; Williard, K.W.; Schoonover, J.E. Fundamentals of watershed hydrology. *J. Contemp. Water Res. Educ.* **2015**, *154*, 3–20. [CrossRef]
25. Davie, T.; Quinn, N.W. *Fundamentals of Hydrology*; Routledge: Oxon, UK; New York, NY, USA, 2019.
26. Raghunath, H.M. *Hydrology: Principles, Analysis and Design*; New Age International: New Delhi, India, 2006.
27. EU. *Guidance Document on the Application of Water Balances for Supporting the Implementation of the WFD*; European Union Technical Report; EU: Luxembourg, 2015; ISBN 978-92-79-52021-1.
28. McKee, T.B.; Doesken, N.J.; Kleist, J. The relationship of drought frequency and duration to time scales. In Proceedings of the 8th Conference on Applied Climatology, Boston, MA, USA, 17–22 January 1993.
29. Eslamian, S.; Ostad-Ali-Askari, K.; Singh, V.P.; Dalezios, N.R.; Ghane, M.; Yihdego, Y.; Matouq, M. A review of drought indices. *Int. J. Constr. Res. Civ. Eng. (Ijrcre)* **2017**, *3*, 48–66.
30. Mishra, A.K.; Singh, V.P. A review of drought concepts. *J. Hydrol.* **2010**, *391*, 202–216. [CrossRef]
31. Tigkas, D.; Vangelis, H.; Tsakiris, G. DrinC: A software for drought analysis based on drought indices. *Earth Sci. Inform.* **2015**, *8*, 697–709. [CrossRef]
32. Anderson, M.C.; Kustas, W.P.; Norman, J.M.; Hain, C.R.; Mecikalski, J.R.; Schultz, L.; González-Dugo, M.; Cammalleri, C.; d'Urso, G.; Pimstein, A. Mapping daily evapotranspiration at field to continental scales using geostationary and polar orbiting satellite imagery. *Hydrol. Earth Syst. Sci.* **2011**, *15*, 223–239. [CrossRef]
33. Zhang, Y.; Peña-Arancibia, J.L.; McVicar, T.R.; Chiew, F.H.; Vaze, J.; Liu, C.; Lu, X.; Zheng, H.; Wang, Y.; Liu, Y.Y. Multi-decadal trends in global terrestrial evapotranspiration and its components. *Sci. Rep.* **2016**, *6*, 19124. [CrossRef]
34. McCabe, M.; Ershadi, A.; Jimenez, C.; Miralles, D.G.; Michel, D.; Wood, E.F. The GEWEX LandFlux project: Evaluation of model evaporation using tower-based and globally-gridded forcing data. *Geosci. Model Dev.* **2016**, *9*, 283–305. [CrossRef]
35. MEFCC. *Towards a Water Managmentprogram for the Awash River Basin*; Ethiopian Ministry of Environment, Forest and Climate Change; Centre for Science and Environmnet (CSE): Addis Ababa, Ethiopia, 2018.
36. Yibeltal, T.; Belte, B.; Semu, A.; Imeru, T.; Yohannes, T. *Coping with Water Scarcity, the Role of Agriculture, Developing a Water Audit for Awash River Basin, Synthesis Report*; GCP/INT/072/ITA; Ministry of Water and Energy (MoWE) and FAO: Addis Ababa, Ethiopia, December 2013.

37. Tadese, M.; Kumar, L.; Koech, R.; Kogo, B.K. Mapping of land-use/land-cover changes and its dynamics in Awash River Basin using remote sensing and GIS. *Remote Sens. Appl. Soc. Environ.* **2020**, *19*, 100352. [CrossRef]
38. Hijmans, R.J.; Cameron, S.E.; Parra, J.L.; Jones, P.G.; Jarvis, A. Very high resolution interpolated climate surfaces for global land areas. *Int. J. Climatol. A J. R. Meteorol. Soc.* **2005**, *25*, 1965–1978. [CrossRef]
39. Tadese, M.T.; Kumar, L.; Koech, R. Climate Change Projections in the Awash River Basin of Ethiopia using Global and Regional Climate Models. *Int. J. Climatol.* **2020**, *40*, 3649–3666. [CrossRef]
40. Hargreaves, G.H. Defining and using reference evapotranspiration. *J. Irrig. Drain. Eng.* **1994**, *120*, 1132–1139. [CrossRef]
41. Tsakiris, G.; Pangalou, D.; Vangelis, H. Regional drought assessment based on the Reconnaissance Drought Index (RDI). *Water Resour. Manag.* **2007**, *21*, 821–833. [CrossRef]
42. Tigkas, D.; Vangelis, H.; Tsakiris, G. Implementing Crop Evapotranspiration in RDI for Farm-Level Drought Evaluation and Adaptation under Climate Change Conditions. *Water Resour. Manag.* **2020**, 1–15. [CrossRef]
43. Tsakiris, G.; Vangelis, H. Establishing a drought index incorporating evapotranspiration. *Eur. Water* **2005**, *9*, 3–11.
44. Tigkas, D. Drought characterisation and monitoring in regions of Greece. *Eur. Water* **2008**, *23*, 29–39.
45. Tsakiris, G.; Nalbantis, I.; Pangalou, D.; Tigkas, D.; Vangelis, H. Drought meteorological monitoring network design for the reconnaissance drought index (RDI). In Proceedings of the 1st International Conference "Drought Management: Scientific and Technological Innovations" Option Méditerranéennes, Series A, No. 80, Zaragoza, Spain, 12–14 June 2008; pp. 57–62.
46. Edossa, D.C.; Babel, M.S.; Gupta, A.D. Drought analysis in the Awash river basin, Ethiopia. *Water Resour. Manag.* **2010**, *24*, 1441–1460. [CrossRef]
47. Gebrehiwot, T.; van der Veen, A.; Maathuis, B. Spatial and temporal assessment of drought in the Northern highlands of Ethiopia. *Int. J. Appl. Earth Obs. Geoinf.* **2011**, *13*, 309–321. [CrossRef]
48. Shah, R.; Bharadiya, N.; Manekar, V. Drought index computation using standardized precipitation index (SPI) method for Surat District, Gujarat. *Aquat. Procedia* **2015**, *4*, 1243–1249. [CrossRef]
49. Tan, C.; Yang, J.; Li, M. Temporal-spatial variation of drought indicated by SPI and SPEI in Ningxia Hui Autonomous Region, China. *Atmosphere* **2015**, *6*, 1399–1421. [CrossRef]
50. Khalili, D.; Farnoud, T.; Jamshidi, H.; Kamgar-Haghighi, A.A.; Zand-Parsa, S. Comparability analyses of the SPI and RDI meteorological drought indices in different climatic zones. *Water Resour. Manag.* **2011**, *25*, 1737–1757. [CrossRef]
51. Nalbantis, I.; Tsakiris, G. Assessment of hydrological drought revisited. *Water Resour. Manag.* **2009**, *23* 881–897. [CrossRef]
52. Tsakiris, G.; Vangelis, H. Towards a drought watch system based on spatial SPI. *Water Resour. Manag.* **2004**, *18*, 1–12. [CrossRef]
53. UNEP. *World Atlas of Desertification*, 2nd ed.; Arnold: New York, NY, USA, 1997.
54. Gizaw, M.S.; Biftu, G.F.; Gan, T.Y.; Moges, S.A.; Koivusalo, H. Potential impact of climate change on streamflow of major Ethiopian rivers. *Clim. Chang.* **2017**, *143*, 371–383. [CrossRef]
55. Seleshi, Y.; Zanke, U. Recent changes in rainfall and rainy days in Ethiopia. *Int. J. Climatol.* **2004**, *24*, 973–983. [CrossRef]
56. Yadeta, D.; Kebede, A.; Tessema, N. Climate change posed agricultural drought and potential of rainy season for effective agricultural water management, Kesem sub-basin, Awash Basin, Ethiopia. *Theor. Appl. Climatol.* **2020**, *140*, 653–666. [CrossRef]
57. Getahun, Y.S.; Li, M.-H.; Chen, P.-Y. Assessing Impact of Climate Change on Hydrology of Melka Kuntrie Subbasin, Ethiopia with Ar4 and Ar5 Projections. *Water* **2020**, *12*, 1308. [CrossRef]
58. Taye, M.; Dyer, E.; Hirpa, F.; Charles, K. Climate Change Impact on Water Resources in the Awash Basin, Ethiopia. *Water* **2018**, *10*, 1560. [CrossRef]
59. Tadese, M.T.; Kumar, L.; Koech, R.; Zemadim, B. Hydro-Climatic Variability: A Characterisation and Trend Study of the Awash River Basin, Ethiopia. *Hydrology* **2019**, *6*, 35. [CrossRef]

60. VividEconomics. Water resources and extreme events in the Awash basin: Economic effects and policy implications, Report. In *Vivid Economics*; Smale, R., Hope, R., Charles, K., Hall, J., Dadson, S., Borgomeo, E., Kebede, S., Alamire, T., Bekele, F., Eds.; Report Prepared for the Global Green Growth Institute, Ethiopia; VividEconomics: London, UK, April 2016.
61. Adnew Degefu, M.; Assen, M.; Satyal, P.; Budds, J. Villagization and access to water resources in the Middle Awash Valley of Ethiopia: Implications for climate change adaptation. *Clim. Dev.* **2019**, 1–12. [CrossRef]